Signatures of Quantum-like Chaos in Spacing Intervals of Non-trivial Riemann Zeta Zeros and in Turbulent Fluid Flows

A. M. Selvam

(Retired) Indian Institute of Tropical Meteorology

Pune 411 008, India

email: selvam@ip.eth.net

website: http://www.geocities.com/amselvam

The spacing intervals of adjacent Riemann zeta zeros (non-trivial) exhibit fractal (irregular) fluctuations generic to dynamical systems in nature such as fluid flows, heart beat patterns, stock market price index, etc., and are associated with unpredictability or chaos. The power spectra of such fractal space-time fluctuations exhibit inverse power-law form and signify long-range correlations, identified as *self-organized criticality*. A cell dynamical system model developed by the author for turbulent fluid flows provides a unique quantification for the observed power spectra in terms of the statistical normal distribution, such that the variance represents the statistical probability densities. Such a result that the additive amplitudes of eddies when squared, represent the statistical probabilities is an observed feature of the subatomic dynamics of quantum systems such as an electron or photon. *Self-organized* criticality is therefore a signature of quantum-like chaos in dynamical systems. The model

concepts are applicable to all real world (observed) and computed (mathematical model) dynamical systems.

Continuous periodogram analyses of the fractal fluctuations of Riemann zeta zero spacing intervals show that the power spectra follow the unique and universal inverse power-law form of the statistical normal distribution. The Riemann zeta zeros therefore exhibit quantum-like chaos, the spacing intervals of the zeros representing the energy (variance) level spacings of quantum-like chaos inherent to dynamical systems in nature. The cell dynamical system model is a general systems theory applicable to dynamical systems of all size scales.

Keywords: fractal structure of spacing intervals of Riemann zeta zeros, quantum-like chaos in Riemann zeta zeros, self-organized criticality in Riemann zeta zeros

1.　Introduction

The Riemann zeta function $z(s)$ is a function of the complex variable s ($=x+iy$) and is defined as a sum over all integers (Keating, 1990)

$$z(s) = 1 + 1/2^s + 1/3^s + 1/4^s + 1/5^s + ...if\ x > 1 \qquad (1)$$

The analytic properties of the zeta function are also related to the distribution of prime numbers. It is known that there are an infinite number of prime numbers. Though the prime numbers appear to be distributed at random among the integers, the distribution follows the approximate law that the number of primes $p(x)$ up to the integer x is equal to $x/logx$ where log is the natural logarithm. The actual distribution of primes fluctuates on either side of the estimated value and approach closely the estimated value for large values of x.

In 1859 Bernhard Riemann gave an exact formula for the counting function $p(x)$, in which fluctuations about the average are related to the value of s for which $z(s) = 0$, s being a complex number. Based on a few numerical computations Riemann conjectured that an important set of the zeros, namely the non-trivial zeros, all have real part equal to $x = 1/2$. This is the Riemann hypothesis (Keating, 1990; Devlin, 1997). Numerical computations done so far agree with Riemann's hypothesis. However, a theoretical proof will establish the validity of numerous results in number theory, which assume that the Riemann hypothesis is true.

A proof of Riemann hypothesis will also help physicists to compute the chaotic orbits of complex atomic systems such as a hydrogen atom in a magnetic field, to the oscillations of large nuclei (Richards, 1988; Gutzwiller, 1990; Berry, 1992; Cipra, 1996; Klarreich, 2000). It is now believed that the spectrum of Riemann zeta zeros represent the energy spectrum of complex quantum systems which exhibit classical chaos.

A cell dynamical system model developed by the author shows that quantum-like chaos is inherent to fractal space-time fluctuations exhibited by dynamical systems in nature ranging from sub-atomic and molecular scale quantum systems to macro-scale turbulent fluid flows. The model provides a unique quantification for the fractal fluctuations in terms of the statistical normal distribution. The Riemann zero spacing intervals exhibit fractal fluctuations and the power spectrum exhibits model predicted universal inverse power-law form of the statistical normal distribution. The distribution of Riemann zeros therefore exhibit quantum-like chaos.

2.   Cell Dynamical System Model

As mentioned earlier (Section 1: Introduction) power spectral analyses of fractal space-time fluctuations exhibit inverse power-law form, *i.e.*, a self-similar eddy continuum. The cell dynamical system model (Mary Selvam, 1990; Selvam and Fadnavis, 1998, and all references contained therein) is a general systems theory (Capra, 1996) applicable to dynamical systems of all size scales. The model shows that such an eddy continuum can be visualised as a hierarchy of successively larger scale eddies enclosing smaller scale eddies. An eddy or wave is characterised by circulation speed and radius. Large eddies of root mean square (r.m.s) circulation speed W and radius R form as envelopes enclosing small eddies of r.m.s circulation speed w_* and radius r such that

$$W^2 = \frac{2}{P} \frac{r}{R} w_*^2$$
(2)

Large eddies are visualised to grow at unit length step increments at unit intervals of time, the units for length and time scale increments being respectively equal to the enclosed small eddy perturbation length scale r and the corresponding eddy circulation time scale.

Since the large eddy is but the average of the enclosed smaller eddies, the eddy energy spectrum follows the statistical normal distribution according to the *Central Limit Theorem* (Ruhla, 1992). Therefore, the variance represents the probability densities. Such a result that the additive amplitudes of the eddies when squared, represent the probabilities is an observed feature of the subatomic dynamics of quantum systems such as the electron or photon (Maddox 1988a, 1993; Rae, 1988). The fractal space-time fluctuations exhibited by dynamical systems are signatures of quantum-like mechanics. The cell dynamical system model provides a unique quantification for the apparently chaotic or unpredictable

nature of such fractal fluctuations (Selvam and Fadnavis, 1998). The model predictions for quantum-like chaos of dynamical systems are as follows. (a) The observed fractal fluctuations of dynamical systems are generated by an overall logarithmic spiral trajectory with the quasiperiodic *Penrose* tiling pattern for the internal structure. (b) Conventional continuous periodogram power spectral analyses of such spiral trajectories will reveal a continuum of periodicities with progressive increase in phase. (c) The broadband power spectrum will have embedded dominant wavebands, the bandwidth increasing with period length. The peak periods (or length scales) E_n in the dominant wavebands are given by the relation

$$E_n = T_s (2 + t) t^n \qquad (3)$$

where t is the golden mean equal to *(1+√5)/2 [@ 1.618]* and T_s, the primary perturbation length scale. Considering the most representative example of turbulent fluid flows, namely, atmospheric flows, Ghil (1994) reports that the most striking feature in climate variability on all time scales is the presence of sharp peaks superimposed on a continuous background. The model predicted periodicities (or length scales) in terms of the primary perturbation length scale units are *2.2*, *3.6*, *5.8*, *9.5*, *15.3*, *24.8*, *40.1*,and *64.9* respectively for values of *n* ranging from *–1* to *6*. Periodicities close to model predicted have been reported in weather and climate variability (Burroughs 1992; Kane 1996). (d) The ratio *r/R* also represents the increment dq in phase angle q (Equation 2). Therefore the phase angle q represents the variance. Hence, when the logarithmic spiral is resolved as an eddy continuum in conventional spectral analysis, the increment in wavelength is concomitant with increase in phase (Selvam and Fadnavis, 1998). Such a result that increments in wavelength and phase angle are related is observed in quantum systems and has been named '*Berry's phase*' (Berry 1988;

Maddox 1988b; Simon *et al*., 1988; Anandan, 1992). The relationship of angular turning of the spiral to intensity of fluctuations is seen in the tight coiling of the hurricane spiral cloud systems. The overall logarithmic spiral flow structure is given by the relation

$$W = \frac{w_*}{k} log\, z \qquad (4)$$

where the constant *k* is the steady state fractional volume dilution of large eddy by inherent turbulent eddy fluctuations. The constant *k* is equal to $1/t^2 (@0.382)$ and is identified as the universal constant for deterministic chaos in fluid flows (Selvam and Fadnavis, 1998). The steady state emergence of fractal structures is therefore equal to

$$1/k\ @\ 2.62 \qquad (5)$$

The model predicted logarithmic wind profile relationship such as Equation 4 is a long-established (observational) feature of atmospheric flows in the boundary layer, the constant *k*, called the *Von Karman*'s constant has the value equal to *0.38* as determined from observations (Hogstrom, 1985).

In Equation 4, *W* represents the standard deviation of eddy fluctuations, since *W* is computed as the instantaneous r.m.s. (root mean square) eddy perturbation amplitude with reference to the earlier step of eddy growth. For two successive stages of eddy growth starting from primary perturbation w_* the ratio of the standard deviations W_{n+1} and W_n is given from Equation 4 as *(n+1)/n*. Denoting by **s**, the standard deviation of eddy fluctuations at the reference level (*n=1*), the standard deviations of eddy fluctuations for successive stages of eddy growth are given as integer multiple of **s**, *i.e.*, **s**, *2***s**, *3***s**, etc. and correspond respectively to

statistical normalized stan dard deviation t = 0,1,2,3,etc.   (6)

The conventional power spectrum plotted as the variance versus the frequency in log-log scale will now represent the eddy probability density on logarithmic scale versus the standard deviation of the eddy fluctuations on linear scale since the logarithm of the eddy wavelength represents the standard deviation, *i.e.*, the r.m.s. value of eddy fluctuations (Equation 4). The r.m.s. value of eddy fluctuations can be represented in terms of statistical normal distribution as follows. A normalized standard deviation $t=0$ corresponds to cumulative percentage probability density equal to *50* for the mean value of the distribution. Since the logarithm of the wavelength represents the r.m.s. value of eddy fluctuations the normalized standard deviation t is defined for the eddy energy as

$$t = (log\ L/log\ T_{50}) - 1 \qquad (7)$$

where L is the period in years and T_{50} is the period up to which the cumulative percentage contribution to total variance is equal to *50* and $t = 0$. The variable $Log T_{50}$ also represents the mean value for the r.m.s. eddy fluctuations and is consistent with the concept of the mean level represented by r.m.s. eddy fluctuations. Spectra of time series of fluctuations of dynamical systems, for example, meteorological parameters, when plotted as cumulative percentage contribution to total variance versus t follow the model predicted universal spectrum (Selvam and Fadnavis, 1998, and all references therein). The literature shows many examples of pressure, wind and temperature whose shapes display a remarkable degree of universality (Canavero and Einaudi, 1987).

The periodicities (or length scales) T_{50} and T_{95} up to which the cumulative percentage contribution to total variances are respectively equal to *50* and *95* are computed from model concepts as follows.

The power spectrum, when plotted as normalised standard deviation t versus cumulative percentage contribution to total variance

represents the statistical normal distribution (Equation 7), *i.e.*, the variance represents the probability density. The normalised standard deviation values *t* corresponding to cumulative percentage probability densities *P* equal to *50* and *95* respectively are equal to *0* and *2* from statistical normal distribution characteristics. Since *t* represents the eddy growth step *n* (Equation 6) the dominant periodicities (or length scales) T_{50} and T_{95} up to which the cumulative percentage contribution to total variance are respectively equal to *50* and *95* are obtained from Equation 3 for corresponding values of *n* equal to *0* and *2*. In the present study of fractal fluctuations of spacing intervals of adjacent Riemann zeta zeros, the primary perturbation length scale T_s is equal to unit spacing interval and T_{50} and T_{95} are obtained as

$$T_{50} = (2+t)\, t^{\,0} \; @ \; 3.6 \text{unit spacing intervals} \tag{8}$$

$$T_{95} = (2+t)\, t^{\,2} \; @ \; 9.5 \text{unit spacing intervals} \tag{9}$$

3.   Data and Analysis

Details of the Riemann zeta zeros (non-trivial) used in the present study are given in the following:

(a)   The first 100000 zeros were obtained from:
http://www.research.att.com/~amo/zeta_tables/zeros1

(b)   Riemann zeta zeros numbered $10^{12} + 1$ through $10^{12} + 10^4$ were obtained from:
http://www.research.att.com/~amo/zeta_tables/zeros3

[Values of gamma - 267653395647, where gamma runs over the heights of the zeros of the Riemann zeta numbered $10^{12} + 1$ through $10^{12} + 10^4$. Thus

zero # $10^{12} + 1$ is actually

1/2 + i * 267,653,395,648.8475231278...

Values are guaranteed to be accurate only to within 10^{-8}].

(c)   Riemann zeta zeros numbered $10^{21} + 1$ through $10^{21} + 10^4$ were obtained from:

http://www.research.att.com/~amo/zeta_tables/zeros4

[Values of gamma - 144176897509546973000, where gamma runs over the heights of the zeros of the Riemann zeta numbered $10^{21} + 1$ through $10^{21} + 10^4$.

Thus zero # $10^{21} + 1$ is actually

$1/2 + i * 144,176,897,509,546,973,538.49806962...$

Values are not guaranteed, and are probably accurate to within 10^{-6}].

(d)   Riemann zeta zeros numbered $10^{22} + 1$ through $10^{22} + 10^4$ were obtained from:

http://www.research.att.com/~amo/zeta_tables/zeros5

[Values of gamma - 1370919909931995300000, where gamma runs over the heights of the zeros of the Riemann zeta numbered $10^{22} + 1$ through $10^{22} + 10^4$.

Thus zero # $10^{22} + 1$ is actually

$1/2 + i * 1,370,919,909,931,995,308,226.68016095...$

Values are not guaranteed, and are probably accurate to within 10^{-6}].

3.1   Fractal structure of spacing intervals of adjacent Riemann zeta zeros

The spacing interval between adjacent zeta zeros for a representative sample of *100* successive zeta zeros starting from the *80,000*th value are plotted in Figure 1. The irregular zig-zag pattern of fluctuations of adjacent spacing intervals is identified as characteristic of fractal fluctuations exhibited by dynamical systems, such as, rainfall, river flows, stock market price index, etc. (Selvam and Fadnavis, 1998).

Figure 1

fractal structure of spacing interval

between adjacent zeta zeros

100 zeta zeros starting from 80000th
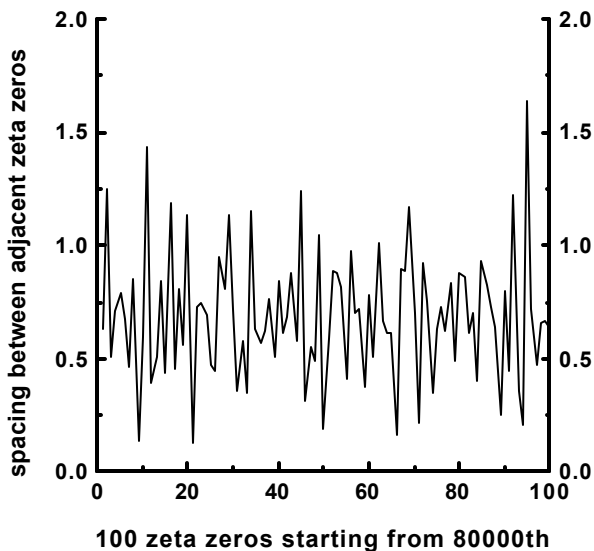
the first 100000 non-trivial zeta zeros were obtained from
http://www.research.att.com/~amo/zeta_tables/zeros1
100 zeta zeros starting from 80000th value

3.2   Continuous periodogram analyses of fractal structure of spacing intervals of adjacent Riemann zeta zeros

The broadband power spectrum of space-time fluctuations of dynamical systems can be computed accurately by an elementary, but very powerful method of analysis developed by Jenkinson (1977) which provides a quasi-continuous form of the classical periodogram allowing systematic allocation of the total variance and degrees of freedom of the data series to logarithmically spaced elements of the frequency range (0.5, 0). The periodogram is constructed for a fixed set of *10000(m)* periodicities L_m which increase geometrically as $L_m = 2\ exp(Cm)$ where *C=.001* and *m=0, 1, 2,....m* . The data series Y_t for the *N* data points was used. The periodogram estimates the set of $A_m cos(2\boldsymbol{pn}_m S\text{-}\boldsymbol{f}_m)$ where A_m, $\boldsymbol{n}_m$ and $\boldsymbol{f}_m$ denote respectively the amplitude, frequency and phase angle for the mth periodicity and *S* is the time or space interval. In the present study the adjacent spacing intervals for different ranges of zeta zeros were used. The cumulative percentage contribution to total variance was computed starting from the high frequency side of the spectrum. The period T_{50} at which *50%* contribution to total variance occurs is taken as reference and the normalized standard deviation t_m values are computed as (Equation 7).

$$t_m = (\,log\ L_m\,/log\ T_{50}\,) - 1$$

The cumulative percentage contribution to total variance, the cumulative percentage normalized phase (normalized with respect to the total phase rotation) and the corresponding *t* values were computed. The power spectra were plotted as cumulative percentage contribution to total variance versus the normalized standard

deviation t as given above. The period L is in units of number of class intervals, unit class interval being equal to adjacent spacing interval of zeta zeros in the present study. Periodicities up to T_{50} contribute up to *50%* of total variance. The phase spectra were plotted as cumulative percentage normalized (normalized to total rotation) phase .

Five groups of data sets (*zeros5*, *zeros4*, *zeros3*, *zeros1a* and *zeros1b*) were used. Details of these five data sets are: (i) The first three data groups, namely, *zeros5*, *zeros4*, *zeros3* consist of the following thirteen data sets of the same length located at same locations in the three data files *zeros5*, *zeros4*, and *zeros3* respectively (1) 1 to100 (2) 1 to 500 (3) 1 to 1000 (4) 1 to 1500 (5) 1 to 2000 (6) 1 to 3000 (7) 1 to 4000 (8) 1 to 5000 (9) 5000 to 5099 (10) 5000 to 5499 (11) 5000 to 5999 (12) 5000 to 6499 (13) 1 to 9999. (ii) The data group *zeros1a* consists of the first twelve data sets shown above for the first three data groups at corresponding locations in data file *zeros1*. (iii) The data group *zeros1b* consists of the following eight data sets located in data file *zeros1* (1) 5000 to 14999 (2) 5000 to 9999 (3) 10000 to 19999 (4) 80000 to 89999 (5) 80000 to 80099 (6) 98000 to 98049 (7) 98009 to 98049 (8) file *zeros3*, 5000 to 5049.

The results of power spectral analyses for all the data sets are shown in Figures 2 to 9. The variance and phase spectra along with statistical normal distributions are shown in Figures 2 and 3 for two representative data sets of Riemann zeta zero spacing intervals. Also, for these two representative data sets, the cumulative percentage contribution to total variance and the cumulative (%) normalized phase (normalized with respect to. the total rotation) for each dominant waveband is computed for significant wavebands and shown in Figures 4 and 5 to illustrate *Berry's phase*, namely the progressive increase in phase with increase in period and also the close association between phase and variance (see Section 2)

Figure 6 shows the following: (a) details of data files (b) data series location in the data file (c) number of data values in each series (d) the value of T_{50} which is the length scale up to which the cumulative percentage contribution to total variance is equal to *50* (in unit spacing intervals of Riemann zeta zeros). (e) whether the variance and phase spectra follow statistical normal distribution characteristics. The length of the data sets ranged from *50 to 10,000* values.

Figures 7 to 9 give the following additional results for the same data sets grouped according to frequency of occurrence of dominant wavebands with peak periodicities in class intervals *2 - 3*, *3 - 4*, *4 - 6*, *6 - 12*, *12 - 20*, *20 - 30*, *30 - 50*, *50 – 80.* These wavebands include the model predicted (Equation 3) dominant peak periodicities (or length scales) *2.2*, *3.6*, *5.8*, *9.5*, *15.3*, *24.8*, *40.1*, and *64.9* (in unit spacing intervals of Riemann zeta zeros) for values of *n* ranging from *-1 to 6*. Figures 7a and 7b show the percentage number of dominant wavebands. Figures 8a and 8b show the percentage number of statistically significant (less than or equal to 5% level) dominant wavebands. Figures 9a and 9b show the percentage number of dominant wavebands, which exhibit *Berry's phase*, namely, the variance spectrum follows closely the phase spectrum (see Section 2).

3.3   Results of power spectral analyses

Results of power spectral analyses of Riemann zeta zero spacing intervals agree with the following model predictions: (a) almost all variance spectra follow statistical normal distribution (Figure 6) (b) The magnitude of T_{50} values (Figure 6) are very close to model predicted value of *3.6* unit spacing intervals (see equation 8).

The 'goodness of fit' (statistical chi-square test) between the variance spectrum and statistical normal distribution is significant at less than or equal to *5%* level for the two representative spectra

shown in Figures 2 and 3 and also for almost all the data sets shown by the symbol S in Figure 6. The phase spectrum is close to the statistical normal distribution, but the '*goodness of fit*' is *not* statistically significant in a majority of cases as shown by the symbol N in Figure 6. However, the '*goodness of fit* ' between variance and phase spectra illustrating *Berry's phase* is statistically significant (*chi-square test*) for individual dominant wavebands, particularly for longer periodicities (Figures 4 and 5 and Figures 9a and 9b). The frequency of occurrence of shorter dominant periodicities up to 5 spacing interval units is a maximum as compared to longer periodicities (Figures 7a and 7b). Also a majority of shorter dominant periodicities up to 5 spacing interval units are found to be statistically significant (Figures 8a and 8b). The predominance of shorter dominant periodicities is consistent with model predicted and observed (Figure 6) value of about *3.6* for the value of T_{50} which is the period up to which the cumulative percentage contribution to total variance is equal to *50*.

Figure 2

variance and phase spectra
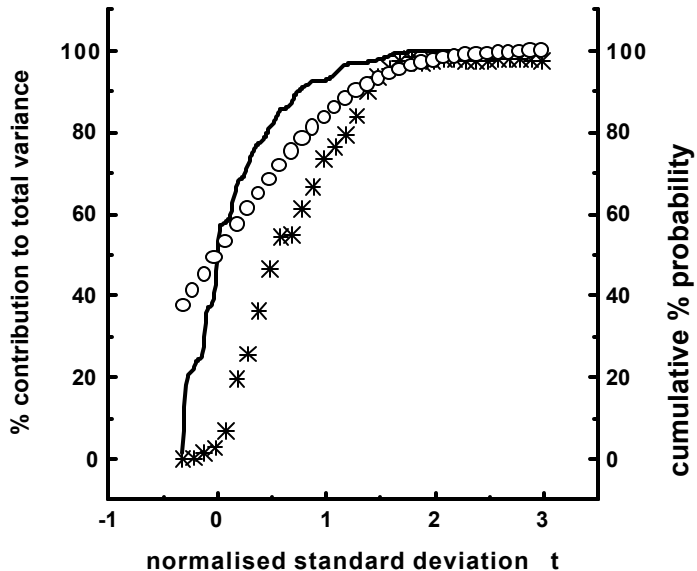
Riemann zeta zeros - 50 values from 98thousandth
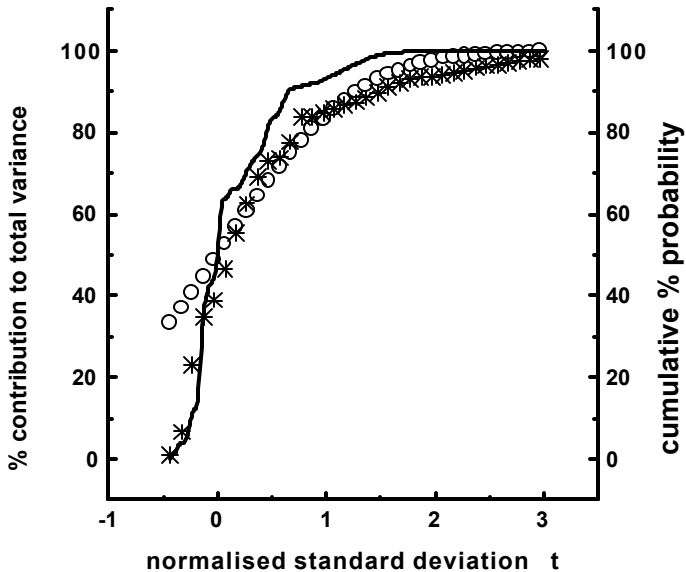
continuous line - variance spectrum

* * * * --> phase spectrum

o o o o --> statistical normal distribution

Riemann nontrivial zeros(first 100000) obtained from

http://www.research.att.com/~amo/zeta_tables/zeros1

variance spectrum follows normal distribution

Figure 3

variance and phase spectra
Riemann zeta zeros - 50 values from 5thousandth

continuous line - variance spectrum
* * * * --> phase spectrum
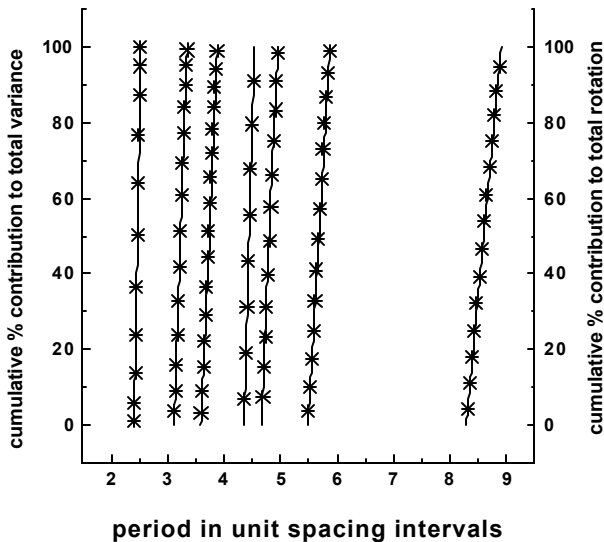**o o o o --> statistical normal distribution**
Riemann nontrivial zeros(10000 values from$10^{12}+1$)
http://www.research.att.com/~amo/zeta_tables/zeros3
variance spectrum follows normal distribution

Figure 4

Berry's phase --- variance and phase spectra
are the same for quantum systems
Riemann zeta zeros - 50 values from 98thousandth

period in unit spacing intervals

continuous line - variance spectrum

* * * * --> phase spectrum

Riemann nontrivial zeros(first 100000) obtained from

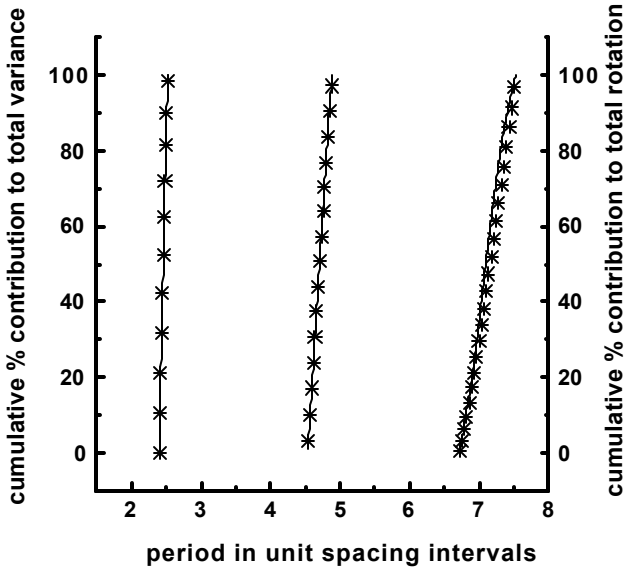http://www.research.att.com/~amo/zeta_tables/zeros1

dominant wave wave bands for which
variance and phase spectra are the same
the goodness of fit being significant at less than 5% level

Figure 5

Berry's phase --- variance and phase spectra

are the same for quantum systems
Riemann zeta zeros - 50 values from 5thousandth

continuous line - variance spectrum

* * * * --> phase spectrum

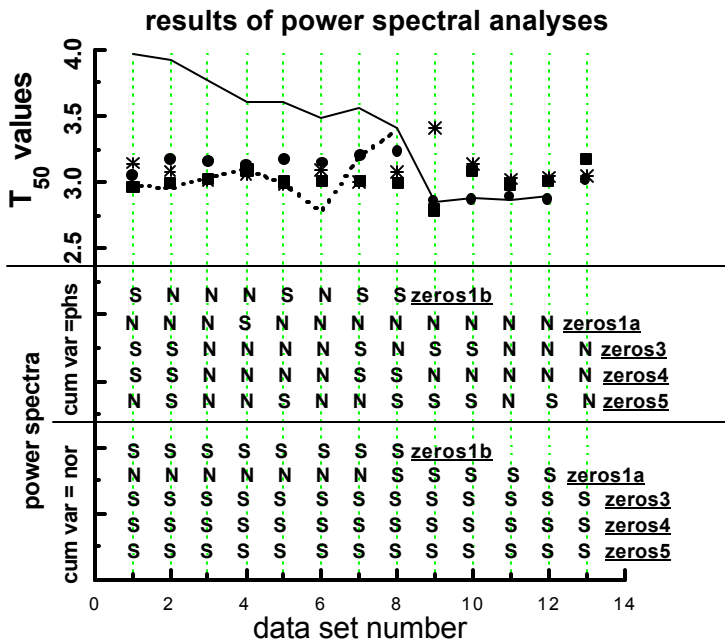**Riemann nontrivial zeros(10000 values from $10^{12}+1$)**
from http://www.research.att.com/~amo/zeta_tables/zeros3
dominant wave bands for which
variance and phase spectra are the same
the goodness of fit being significant at less than 5% level

Figure 6

results of power spectral analyses

DATA SETS -- begin from , number of values

zeros5 ----> solid square   zeros4 ----> solid circle

zeros3 ----> star   zeros1a ----> line

1 ---> 1, 100   2 ---> 1, 500   3 ---> 1, 1000   4 ---> 1, 1500

5 ---> 1, 2000   6 ---> 1, 3000   7 ---> 1, 4000   8 ---> 1, 5000

9 ---> 5000,100   10 ---> 5000,500   11 ---> 5000,1000

12 ---> 5000,1500   13 ---> 1, 9999

zeros1b ----> dot

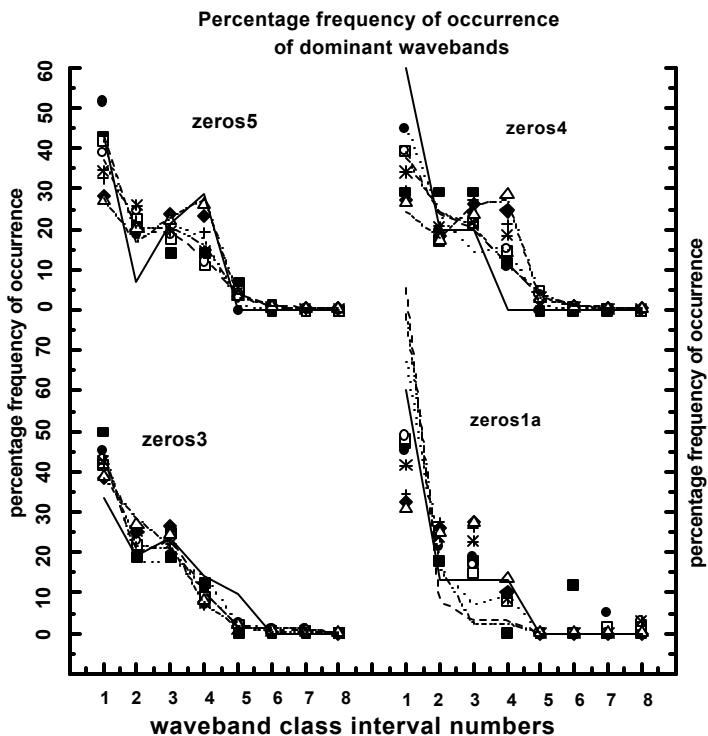1 ----> 5000, 5000   2 -----> 5000, 10000   3 ----> 10000, 10000

4 ----> 80000, 100   5 ----> 80000, 10000   6 ----> 98000, 50

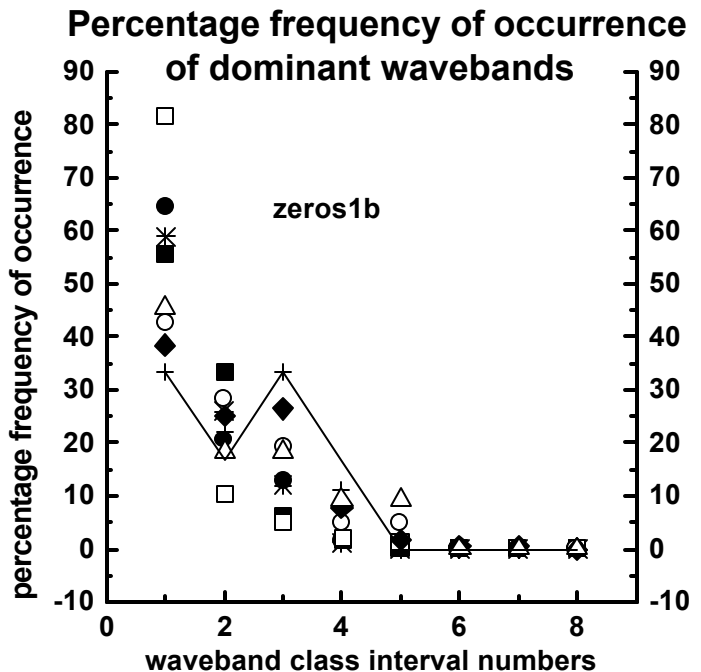7 ----> 98009, 50   8 ----> zeros3, 5000, 50

Figure 7a

Percentage frequency of occurrence of dominant wavebands

zeros5　　zeros4

zeros3　　zeros1a

waveband class interval numbers

DATA SETS -- begin from , number of values

solid square ---> 1, 100 　　 solid circle ------->1, 500

open square ------> 1, 1000 　　 open circle -------> 1, 1500

star ---> 1, 2000 　　 cross ---- > 1, 3000

diamond ---> 1, 4000 　　 open up triangle ---> 1, 5000

line ------> 5000, 100 　　 dot --------> 5000, 500

dash ------> 5000, 1000 　　 ___ .. ___ -------> 5000, 1500

_ . _ ------> 1, 9999

waveband class interval units in terms of 　 adjacent data spacing intervals

1. -----> 2 to 3 　　 2. -----> 3 to 4 　　 3. -----> 4 to 6 　　 4. -----> 6 to12

5. -----> 12 to 20 　　 6. -----> 20 to 30 　　 7. -----> 30 to 50 　　 8. -----> 50 to 80

Figure 7b

Percentage frequency of occurrence of dominant wavebands

zeros1b

percentage frequency of occurrence

waveband class interval numbers

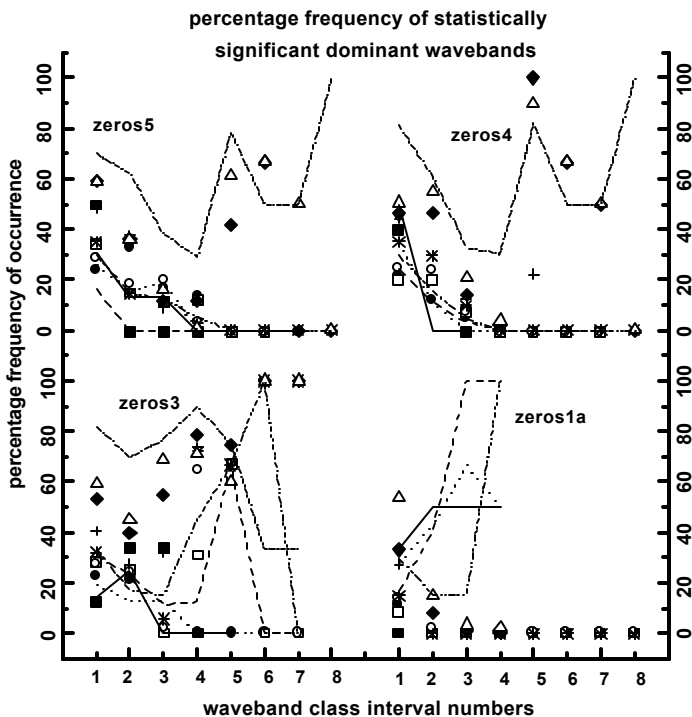**DATA SETS -- begin from , number of values**

solid circle ----> 5000, 5000   open square ----> 80000, 10000

solid square -----> 5000, 10000   cross ----> 98000, 50

star ----> 10000, 10000   up triangle open ----> 98009, 50

open circle ----> 80000, 100   line ----> zeros3, 5000, 50

waveband class interval units in terms of
                              adjacent data spacing intervals

1. -----> 2 to 3   2. -----> 3 to 4   3. -----> 4 to 6

4. -----> 6 to12   5. -----> 12 to 20   6. -----> 20 to 30

7. -----> 30 to 50   8. -----> 50 to 80

Figure 8a

percentage frequency of statistically significant dominant wavebands

DATA SETS -- begin from , number of values

solid square ---> 1, 100
solid circle ----> 1, 500
open square ----> 1, 1000
open circle ----> 1, 1500
star ----> 1, 2000
cross ----> 1, 3000
diamond ----> 1, 4000

open up triangle ----> 1, 5000
line ----> 5000, 100
dot ----> 5000, 500
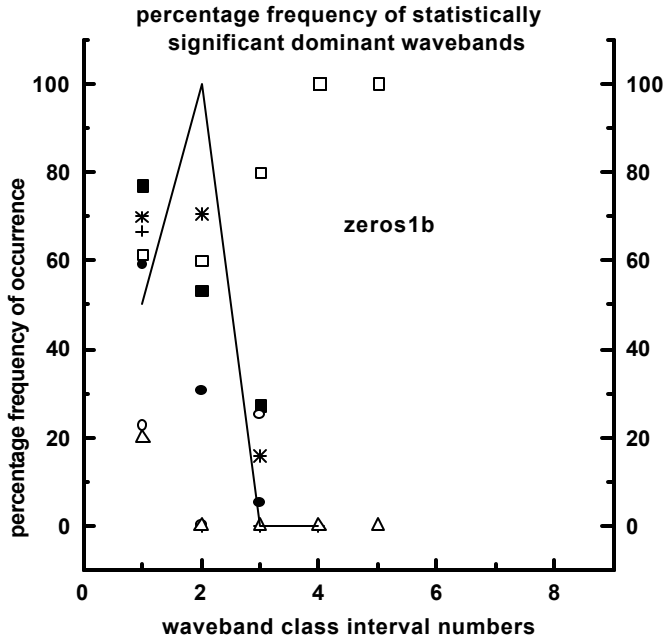dash ----> 5000, 1000
__.__ -----> 5000, 1500
short _._ ----> 1, 9999

waveband class interval units in terms of adjacent data spacing intervals

1. -----> 2 to 3   2. -----> 3 to 4   3. -----> 4 to 6   4. -----> 6 to 12
5. -----> 12 to 20   6. -----> 20 to 30   7. -----> 30 to 50   8. -----> 50 to 80

Figure 8b

percentage frequency of statistically significant dominant wavebands

zeros1b

DATA SETS -- begin from , number of values

solid circle ----> 5000, 5000	open square ----> 80000, 10000
solid square -----> 5000, 10000	cross ----> 98000, 50
star ----> 10000, 10000	up triangle open ----> 98009, 50
open circle ----> 80000, 100	line ----> zeros3, 5000, 50

waveband class interval units in terms of adjacent data spacing intervals

1. -----> 2 to 3	2. -----> 3 to 4	3. -----> 4 to 6
4. -----> 6 to 12	5. -----> 12 to 20	6. -----> 20 to 30
7. -----> 30 to 50	8. -----> 50 to 80	

Figure 9a

percentage of dominant wavebands
which exhibit Berry's phase

DATA SETS -- begin from , number of values

solid square ---> 1, 100	open up triangle ----> 1, 5000
solid circle ----> 1, 500	line ----> 5000, 100
open square ----> 1, 1000	dot ----> 5000, 500
open circle ----> 1, 1500	
star ----> 1, 2000	dash ----> 5000, 1000
cross ----> 1, 3000	__··__ -----> 5000, 1500
diamond ----> 1, 4000	short _·_ ----> 1, 9999

waveband class interval units in terms of adjacent data spacing intervals

1. -----> 2 to 3	2. -----> 3 to 4	3. -----> 4 to 6	4. -----> 6 to 12
5. -----> 12 to 20	6. -----> 20 to 30	7. -----> 30 to 50	8. -----> 50 to 80

Figure 9b

percentage of dominant wavebands which exhibit Berry's phase

zeros1b

y-axis: **percentage frequency of occurrence**

x-axis: **waveband class interval numbers**

DATA SETS -- begin from , number of values

solid circle ----> 5000, 5000   open square ----> 80000, 10000
solid square -----> 5000, 10000   cross ----> 98000, 50
star ----> 10000, 10000   up triangle open ----> 98009, 50
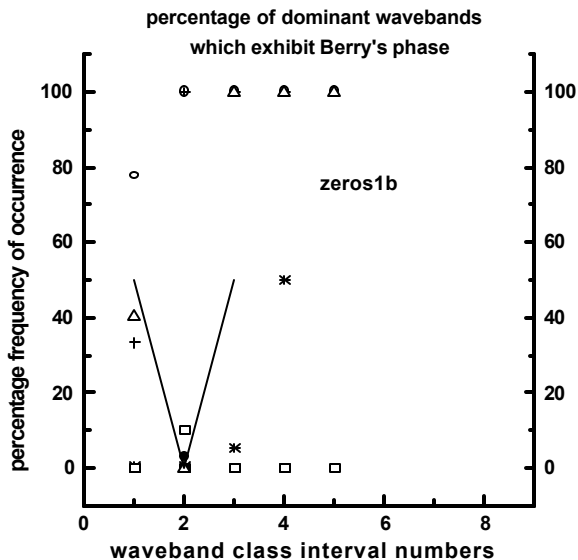open circle ----> 80000, 100   line ----> zeros3, 5000, 50

waveband class interval units in terms of adjacent data spacing intervals

1. -----> 2 to 3   2. -----> 3 to 4   3. -----> 4 to 6
4. -----> 6 to 12   5. -----> 12 to 20   6. -----> 20 to 30
7. -----> 30 to 50   8. -----> 50 to 80

4.   Discussions and Conclusions

The spacing intervals of adjacent Riemann zeta zeros (non-trivial) exhibit fractal fluctuations ubiquitous to dynamical systems in nature (Figure 1). Fractal fluctuations are irregular or chaotic and a search for the physics of their origin has emerged (since 1980s) as a subject of intensive study in the new multidisciplinary science of *Nonlinear Dynamics and Chaos* (Gleick, 1987; Gutzwiller, 1990; Jurgen *et al*., 1990; Bassingthwaighte and Beyer, 1991; Deering and West 1992; Stewart, 1998). Power spectra of fractal fluctuations exhibit inverse power-law form indicating long-range space-time correlations identified as *self-organized criticality* (Bak *et al*., 1987; 1988; Bak and Chen, 1989; 1991; Goldberger *et al*., 1990; Schroeder, 1991; Stanley, 1995; Ghashghaie *et al*., 1996; Buchanan, 1997; Newman, 2000). Also, inverse power-law form for power spectra indicate that an eddy continuum underlies the apparently irregular (or chaotic) fractal fluctuations, *i.e.*, the superimposition of an ensemble of eddies (e.g., such as sine waves) generates the observed fractal fluctuations. A cell dynamical system model developed by the author provides unique quantification for the power spectra of fractal fluctuations in terms of the statistical normal distribution such that the variance represents the probabilities. In summary, fractal fluctuations imply quantum-like chaos in dynamical systems for the following reasons: (a) The superimposition of an ensemble of eddies or waves results in the observed fluctuation pattern. (b) The additive amplitudes of the eddies when squared gives the variance which represents the probability densities. Fractal fluctuations therefore exhibit quantum-like chaos in macro-scale dynamical systems.

Continuous periodogram analyses of Riemann zeta zero spacing intervals show that the power spectra follow the universal and unique inverse power-law form of the statistical normal distribution (Figures

2, 3, 6). Riemann zeta zero spacing intervals therefore exhibit quantum-like chaos and is consistent with similar studies by the author, which have shown that prime number distribution also exhibits quantum-like chaos (Selvam and Fadnavis, 2001; Selvam, 2001). Riemann had shown that the zeta function represents prime number distribution. Observational and computed values of energy level distributions of excited quantum systems appear to follow closely the Riemann zeta zeros and also prime number distribution (Cipra, 1996). The results are consistent with cell dynamical system model prediction that fractal fluctuations are signatures of quantum-like chaos in dynamical systems of all sizes ranging from the sub-atomic quantum systems to macro-scale fluid flows. The Heisenberg uncertainty principle for quantum systems implies unpredictable fluctuations, *i.e.*, fractal space-time fluctuations (Hey and Walters, 1989), which is a signature of quantum-like chaos.

Results of all the data sets (ranging in length from *50 to 10000* values) show that starting from the high frequency side, periodicities up to model predicted value of about *3.6 unit spacing intervals* contribute up to *50%* to the total variance (Figure 6). A possible physical explanation for the observed close relationship between the Riemann zeta zeros and energy levels of quantum systems is given in the following:

The individual fractions *1/2*, *1/3*, *1/4*, *1/5*, etc., in the expression for the Riemann zeta function (Equation 1) may represent (a) the length scale ratio (r/R) of the enclosed primary eddy to the large eddy, which represents the probabilities of occurrence of the primary perturbation in successive growth stages in unit length steps of the large eddy. As shown in Equation 2, this length scale ratio (r/R) represents the variance or eddy energy. Graphically, in the x - y plane (complex plane), the above fractions raised to the power of the complex number *s* ($=x+iy$) represent fractional probabilities

corresponding to the phase angle represented by the location co-ordinates x and y (Argand diagram).

Therefore the Riemann zeta function represents the energy spectrum of quantum systems at any location (x, y). The Riemann zeta zeros on the y-axis at *x=1/2*, therefore represent the eddy energy minima. An angular rotation by 90 degrees of these Riemann zeta zero locations will give the energy (maximum) spectrum of the quantum system. An eddy or wave circulation is bi-directional by concept and is associated with bimodal, namely formation and dissipation respectively of phenomenological form for manifestation of energy (Mary Selvam, 1990). Since manifestation of energy in phenomenological form occurs only in one-half cycle, the corresponding energy levels occur at *x=1/2*.

5.　Acknowledgement

References

Anandan, J., 1992: The geometric phase. *Nature* 360, 307-313.

Bak, P., Tang, C., and Wiesenfeld K., 1987: Self-organized criticality: an explanation of 1/f noise. *Phys. Rev. Lett*. 59, 381-384.

Bak, P.C., Tang, C., and Wiesenfeld, K., 1988: Self-organized criticality. *Phys. Rev. A.* 38, 364 - 374.

Bak, P., Chen, K., 1989: The physics of fractals. *Physica D* 38, 5-12.

Bak, P., Chen, K., 1991: Self-organized criticality. *Sci. Am*., January, 26-33.

Bassingthwaighte, J. B. and Beyer, R. P., 1991: Fractal correlations in heterogeneous systems. *Physica D* 53, 71-84.

Berry, M. V., 1988: The geometric phase. *Sci. Amer*. Dec., 26-32.

Berry, M., 1992: Quantum physics on the edge of chaos. In *The New Scientist's Guide to Chaos*, (Ed) Nina Hall, Penguin Books, pp.184 - 195.

Buchanan, M., 1997: One law to rule them all. *New Scientist* 8 Nov., 30-35.

Burroughs, W. J., 1992: *Weather Cycles: Real or Imaginary*? Cambridge University Press, Cambridge.

Canavero, F. G., Einaudi, F.,1987: Time and space variability of atmospheric processes. *J. Atmos. Sci*. 44(12), 1589-1604.

Capra, F., 1996: *The web of life*, HarperCollins Publishers, London, pp.311.

Cipra, B., 1996: Prime formula weds number theory and quantum physics. *Science* 274, 2014-2015.

Deering, W., and West, B. J., 1992: Fractal physiology. *IEEE Engineering in Medicine and Biology*, June, 40-46.

Devlin, K., 1997: *Mathematics: The Science of Patterns*. Scientific American Library, New York, pp.215.

Ghashghaie, S., Breymann, Peinke, J., Talkner, P., Dodge, Y., 1996: Turbulent cascades in foreign exchange markets. *Nature* 381, 767-770.

Ghil, M., 1994: Cryothermodynamics: the chaotic dynamics of paleoclimate. *Physica D* 77,130-159.

Gleick, J., 1987: *Chaos: Making a New Science*. Viking, New York.

Goldberger, A. L., Rigney, D. R., West, B. J., 1990: Chaos and fractals in human physiology. *Sci. Am*. 262(2), 42-49.

Gutzwiller, M. C., 1990: Chaos in classical and quantum systems. *Interdisciplinary Applied Mathematics*, Volume 1, Springer-Verlag, New York, pp.427.

Hey, T. and Walters, P., 1989: *The quantum universe*. Cambridge University Press, pp.180.

Hogstrom, U., 1985: Von Karman's constant in atmospheric boundary layer now re-evaluated. *J. Atmos. Sci*. 42, 263-270.

Jenkinson, A. F., 1977: *A Powerful Elementary Method of Spectral Analysis for use with Monthly, Seasonal or Annual Meteorological Time Series*. Meteorological Office, London, Branch Memorandum No. 57, pp. 1-23.

Jurgen, H., Peitgen, H-O, Saupe, D., 1990: The language of fractals. Sci. Amer. 263, 40-49.

Keating, J., 1990: Physics and the queen of mathematics. *Physics World* April, 46-50.

Klarreich, E., 2000: Prime time. *New Scientist* 11 November, 32-36.

Maddox, J., 1988a: Licence to slang Copenhagen? *Nature* 332, 581.

Maddox, J., 1988b: Turning phases into frequencies. *Nature* 334, 99.

Maddox, J., 1993: Can quantum theory be understood? *Nature* 361, 493.

Mary Selvam, A., 1990: Deterministic chaos, fractals and quantumlike mechanics in atmospheric flows. Can. J. Phys. 68, 831-841. http://xxx.lanl.gov/html/physics/0010046

Newman, M., 2000: The power of design. *Nature* 405, 412-413.

Rae, A., 1988: *Quantum-physics: illusion or reality?* Cambridge University Press, New York, p.129.

Richards, D., 1988: Order and chaos in strong fields. *Nature* 336, 518-519.

Ruhla, C., 1992: *The physics of chance*. Oxford University Press, Oxford, U. K., pp.217.

Schroeder, M., 1991: *Fractals, Chaos and Powerlaws*. W. H. Freeman and Co., N.Y.

Selvam, A. M., and Fadnavis, S., 1998: Signatures of a universal spectrum for atmospheric interannual variability in some disparate climatic regimes. *Meteorology and Atmospheric Physics* 66, 87-112. http://xxx.lanl.gov/abs/chao-dyn/9805028

Selvam, A. M., and Fadnavis, S., 2001: Cantorian fractal patterns, quantum-like chaos and prime numbers in atmospheric flows.(to be submitted for Journal publication). http://xxx.lanl.gov/abs/chao-dyn/9810011

Selvam, A. M., 2001: Quantum-like chaos in prime number distribution and in turbulent fluid flows. *Apeiron* 8(3), 29-64, (2001). http://redshift.vif.com/ http://xxx.lanl.gov/html/physics/0005067

Simon, R., Kimble, H. J., Sudarshan, E. C. G., 1988: Evolving geometric phase and its dynamical interpretation as a frequency shift: an optical experiment. *Phys. Rev. Letts.* 61(1), 19-22.

Stanley, H. E., 1995: Powerlaws and universality. *Nature* 378, 554.

Stewart, I., 1998: *Life's other secret*. Allen Lane, The penguin press, pp.273.